Vortex dynamics and Compressibility effects in Large-Eddy Simulations (2 of 2)

P. Comte

IMFS, Strasbourg mailto: comte@imfs.u-strasbg.fr

Outline:

- Talk 1
  - Mixing layers (*al.*, J. Silvestrini *et al.*, *Eur. J. Mech. B*, **17**, 1998)
  - LES in Fourier space
  - LES in physical space
  - SGS model assessment
  - Compressible LES formulations
  - Air-intake flow (unpublished)

Outline (cont'd):

- Talk 2
  - spatial discretization
  - High-order conservation schemes
  - MILES ENO assessment
  - example of shock-wave/boundary layer interaction
  - Cavity flows (Y. Dubief)
  - Cavity flows (L. Larchevêque *et al.*, *Phys. Fluids*, *Phys. Fluids*, **15**, 2003, *J. Fluid Mech.*, **516**, 2004)
  - Supersonic compression ramp flows (unpublished)
  - Solid-propellent rocket flow (unpublished)
  - Separation control by tangential blowing (preliminary)
  - Supersonic channel flow (C. Brun *et al.*, ETC5, Toulouse, 2003)
  - MHD mixing layers and jets (H. Baty *et al.*, *Phys. Plasmas*, **10**, 2003)

Acknowledgements

- H. Baty
- E. Briand
- C. Brun
- E. David
- M. Haberkorn
- P. Kessler
- L. Larchevêque
- E. Schwander
- J.H. Silvestrini
- LEGI Grenoble, M. Lesieur, O. Métais
- ONERA Chatillon
- Observatoire de Strasbourg

Spatial discretization (1/2)

- modified wavenumber (Vichnevetsky and Bowles, SIAM, 1982, Lele, J. Comp. Phys., 1992): $k_{mod_q} \in \mathbb{C}$:

$$\widehat{\frac{df}{dx}}(k_q) = i k_{mod_q} \hat{f}(k_q) \; ; \quad k_q = \frac{2\pi}{N\Delta x} q \qquad (1)$$

  - ▷ non-dissipative scheme (*i.e.* purely dispersive) $\Longleftrightarrow k_{mod_q} \in \mathbb{R} \quad \forall q \in [\![-N/2, N/2-1]\!]$

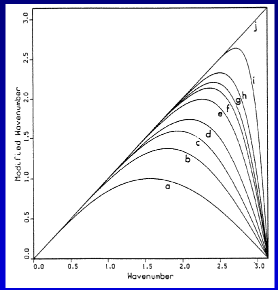

$k_{mod_q}/\Delta x (k_q/\Delta x)$:

a) b) : explicit centered FD, order 2 & 4

c) d) . . . h): compact schemes

j): exact differentiation

Spatial discretization (2/2)

- Compact schemes (for 1st derivatives)
  - ▷ centered schemes

$$\alpha f'_{j-1} + f'_j + \alpha f'_{j+1} = a\frac{f_{j+1} - f_{j-1}}{2\Delta x} + b\frac{f_{j+2} - f_{j-2}}{4\Delta x} + \cdots$$

4th order $\longrightarrow a = \frac{2}{3}(\alpha + 2)$ and $b = \frac{1}{3}(4\alpha - 1)$

  - ◇ explicit: $\alpha = 0 \longrightarrow a = 4/3 \quad b = -1/3$
  - ◇ Pade, Mehrenstellen: $b = 0$ $\longrightarrow \alpha = 1/4 \longrightarrow a = 3/2$
  - ◇ $\alpha = 1/3 \quad a = 14/9 \quad b = 1/9 \longrightarrow$ 6th order

  - ▷ de-centered schemes:

$2f'_{N-1} + f'_N = \dfrac{f_{N-2} - 4f_{N-1} - 5f_N}{2\Delta x}$ and

$f'_1 + 2f'_2 = \dfrac{-5f_1 + 4f_2 + f_3}{2\Delta x}$: 3rd order

Spatial discretization (3/3)

- $\cos'(x)$, 128 points, 8, 16, 32 and 64 periods $\longrightarrow$ integer number of points per period:

16 8 4 2

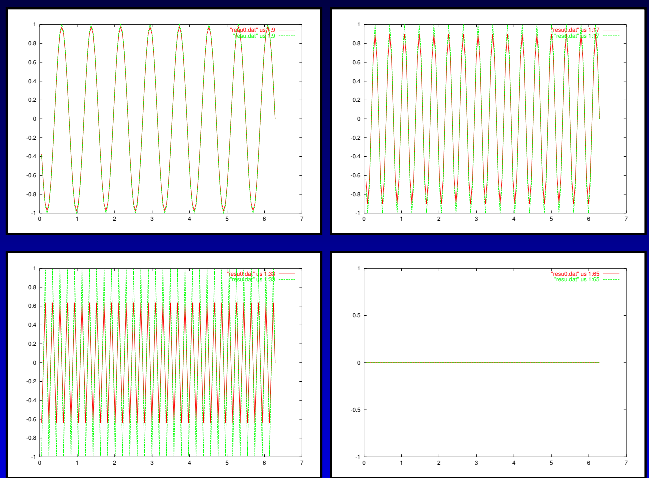

2nd order, 6th order compact

Spatial discretization (4/4)

- $\cos'(x)$, 128 points, 12, 24, and 48 periods $\longrightarrow$ non-integer number of points per period:

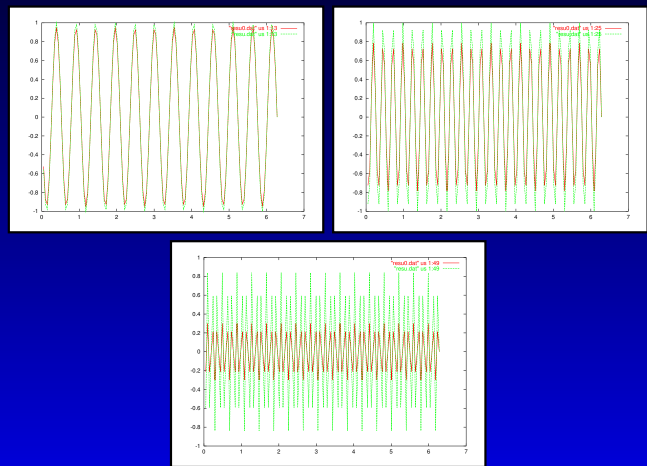

2nd order, 6th order compact.

High-order conservation schemes (1/9)

- since Lax & Wendroff (1960):

$$x_j = j\Delta x, \qquad \frac{\partial u}{\partial t} + \underbrace{\frac{\partial f(u)}{\partial x}}_{\frac{F_{j+\frac12} - F_{j-\frac12}}{\Delta x}} = s(u) \tag{2a}$$

$$\bar{F}_{j+\frac12} = \mathcal{F}(u_{j-q+1}, \ldots, u_j, u_{j+1}, \ldots, u_{j+q}) \tag{2b}$$

$$\mathcal{F}(u, \ldots, u, u, \ldots, u) = f(u) \tag{2c}$$

consistent with weak form, hence with the jump relation across shocks (Rankine-Hugoniot).

High-order conservation schemes (2/9)

- note: for any g piecewise integrable,

$$\frac{g(x+\frac{\Delta x}{2}) - g(x-\frac{\Delta x}{2})}{\Delta x} \equiv \frac{\partial}{\partial x}\underbrace{\left(\frac{1}{\Delta x}\int_{x-\frac{\Delta x}{2}}^{x+\frac{\Delta x}{2}} g(\xi)d\xi\right)}_{\bar{g}(x_j)} . \tag{3}$$

  - ▹ at each grid point: conservative derivation $\equiv$ derivation $\circ$ box-filtering

High-order conservation schemes (3/9)

from now on, assume $g(x_j \pm \frac{\Delta x}{2}) = F_{j\pm\frac12}$.

- with the 2nd order centered scheme:

$$F_{j\pm\frac12} = [f(u_{j\pm1}) + f(u_j)]/2 \qquad ,$$

one has

$$\frac{\partial g}{\partial x} = \frac{g(x+\frac{\Delta x}{2}) - g(x-\frac{\Delta x}{2})}{\Delta x} + \mathcal{O}(\Delta x^2) ,$$

- order $q > 2$ obtained by discrete deconvolution of the box filter

High-order conservation schemes (4/9)

- A_q: approximate inverse of box filter $\bar{}$

$$\frac{\partial g}{\partial x} = \frac{A_q g(x+\frac{\Delta x}{2}) - A_q g(x-\frac{\Delta x}{2})}{\Delta x} + \mathcal{O}(\Delta x^q) , \tag{4}$$

- filter symmetric $\longrightarrow$

$$A_q = 1 + \sum_{p=1}^{p=m} (-1)^p a_{2p} (\Delta x)^{2p} \frac{\partial^{2p}}{\partial x^{2p}} + O(\Delta x)^{2(m+1)} , \tag{5}$$

$m = E(q/2)$: integer part of q, *i.e.*

$q = 2m$ or $q = 2m+1$

- check: $a_2 = 1/24 \qquad a_4 = 7/5760.$

High-order conservation schemes (5/9)

- polynomial A_q can be discretized over several r-point stencils with different degrees of upwinding and stability: $S_k = (x_{j+k-r+1}, x_{j+k-r+2}, \cdots, x_{j+k}),\ k = 0, \cdots, r-1.$
- r^{th}-order-accurate reconstruction $\hat{F}_{j+\frac{1}{2}}$ of the fluxes at interface $j+\frac{1}{2}$:

$$\begin{aligned}\hat{F}_{j+\frac{1}{2}} &= A_r(G(x+\Delta x/2)) \\ &= \sum_{l=0}^{r-1} \alpha^r_{k,l} f(u_{j-r+1+k+l}) \qquad (6)\end{aligned}$$

- $\alpha^r_{k,l}$: reconstruction coefficients

High-order conservation schemes (6/9)

r	k	l=0	l=1	l=2
2	0	-1/2	3/2	
	1	1/2	1/2	
	2	3/2	-1/2	
3	0	1/3	-7/6	11/6
	1	-1/6	5/6	1/3
	2	1/3	5/6	-1/6
	3	11/6	-7/6	1/3

Reconstruction coefficients $\alpha^r_{k,l}$

High-order conservation schemes (7/9)

r	k	l=0	l=1	l=2	l=3	l=4
4	0	-1/4	13/12	-23/12	25/12	
	1	1/12	-5/12	13/12	1/4	
	2	-1/12	7/12	7/12	-1/12	
	3	1/4	13/12	-5/12	1/12	
	4	25/12	-23/12	13/12	-1/4	
5	0	1/5	-21/20	137/60	-163/60	137/60
	1	-1/20	17/60	-43/60	77/60	1/5
	2	1/30	-13/60	47/60	9/20	-1/20
	3	-1/20	9/20	47/60	-13/60	1/30
	4	1/5	77/60	-43/60	17/60	-1/20
	5	137/60	-163/60	137/60	-21/20	1/5

Reconstruction coefficients $\alpha^r_{k,l}$

High-order conservation schemes (8/9)

- check: $r=4$, $k=2$: (6) $\longrightarrow$

$$\begin{aligned}F_{j+\frac{1}{2}} &= \qquad\qquad -\tfrac{1}{12} f_{j-1} + \tfrac{7}{12} f_j + \tfrac{7}{12} f_{j+1} - \tfrac{1}{12} f_{j+2} \\ F_{j-\frac{1}{2}} &= -\tfrac{1}{12} f_{j-2} + \tfrac{7}{12} f_{j-1} + \tfrac{7}{12} f_j - \tfrac{1}{12} f_{j+1}\end{aligned}$$

$$\frac{F_{j+\frac{1}{2}} - F_{j-\frac{1}{2}}}{\Delta x} = \frac{-\frac{1}{12} f_{j-2} - \frac{8}{12} f_{j-1} + \frac{8}{12} f_{j+1} - \frac{1}{12} f_{j+2}}{\Delta x}$$

$$f'_j = -\frac{1}{3}\frac{f_{j+1} - f_{j-1}}{2\Delta x} + \frac{4}{3}\frac{f_{j+2} - f_{j-2}}{4\Delta x}$$

$$\alpha = 0 \quad b = -1/3 \quad a = 4/3$$

$\longrightarrow$ 4th-order centered

High-order conservation schemes (9/9)

r	k	l=0	l=1	l=2	l=3	l=4	l=5	l=6
6	0	-1/6	31/30	-163/60	79/20	-71/20	49/20	
	1	1/30	-13/60	37/60	-21/20	29/20	1/6	
	2	-1/60	7/60	-23/60	19/20	11/30	-1/30	
	3	1/60	-2/15	37/60	37/60	-2/15	1/60	
	4	-1/30	11/30	19/20	-23/60	7/60	-1/60	
	5	1/6	29/20	-21/20	37/60	-13/60	1/30	
	6	49/20	-71/20	79/20	-163/20	31/30	-1/6	
7	0	1/7	-43/42	667/210	-2341/420	853/140	-617/140	363/140
	1	-1/42	37/210	-241/420	153/140	-197/140	233/140	1/7
	2	1/105	-31/420	109/420	-241/420	153/140	13/42	-1/42
	3	-1/140	5/84	-101/420	319/420	107/210	-19/210	1/105
	4	1/105	-19/210	107/210	319/420	-101/420	5/84	-1/140
	5	-1/42	13/42	153/140	-241/420	109/420	-31/420	1/105
	6	1/7	223/140	-197/140	153/140	-241/420	37/210	-1/42
	7	363/140	-617/140	853/140	-2341/420	667/210	-43/42	1/7

Reconstruction coefficients $\alpha^r_{k,l}$

MILES-ENO (1 of 4)

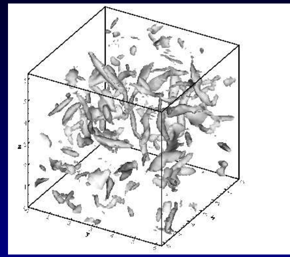
ENO
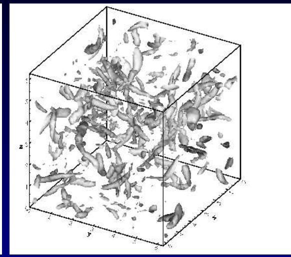
WENO
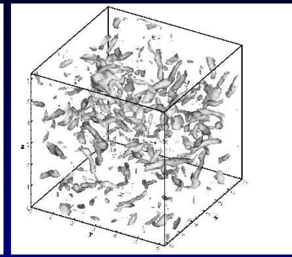
MENO
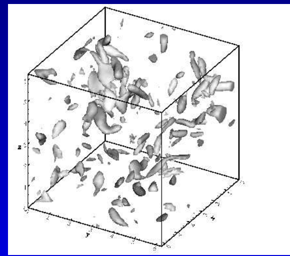
Jameson
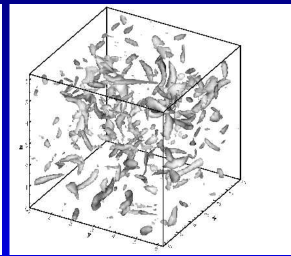
MUSCL4

vorticity magnitude, 64^3 (Garnier *et al.*, J.C.P., 1999):

MILES-ENO (2 of 4)

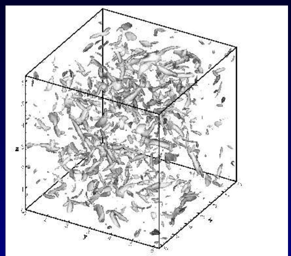
ENO
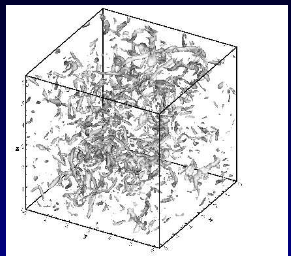
WENO
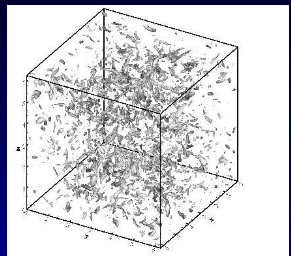
MENO
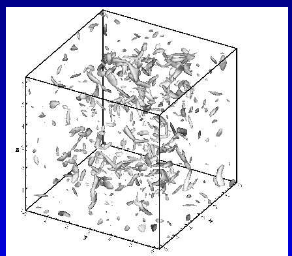
Jameson
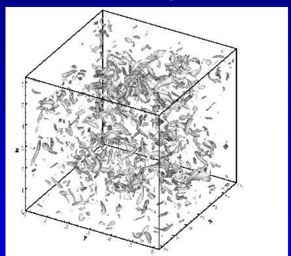
MUSCL4

vorticity magnitude, 128^3 (Garnier *et al.*, J.C.P., 1999):

MILES-ENO (3/4)

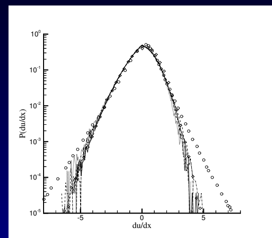
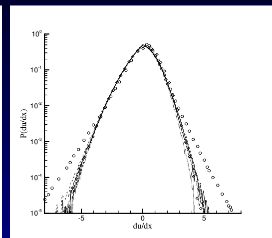

$\partial u/\partial x$ 64^3 128^3

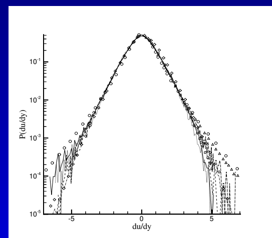
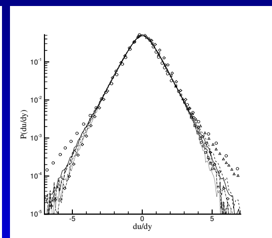

$\partial u/\partial y$ 64^3 128^3

ENO —— WENO – – – MENO –·–·– Jameson —— MUSCL4 – – –

Métais and Lesieur 1992 ($Re_{\bar{\lambda}} \approx 20$) $\Diamond$, She 1991 ($Re_\lambda \approx 24$) $\Box$, She 1991 ($Re_\lambda \approx 77$) $\triangle$,
Vincent and Meneguzzi 1991 ($Rel \approx 150$) $\bigcirc$

MILES-ENO (4/4)

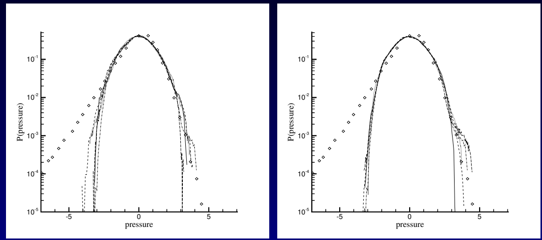

pressure: 64^3 128^3

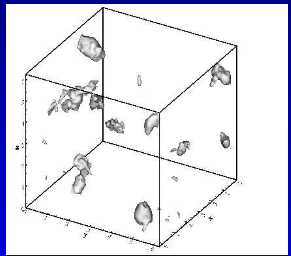

128^3

ENO —— WENO – – – MENO -·-·- Jameson —— MUSCL4 – – –

Métais and Lesieur 1992 ($Re_{\bar{\lambda}} \approx 20$) $\diamondsuit$,

Shock Wave / Boundary Layer Interaction (1 of 1)

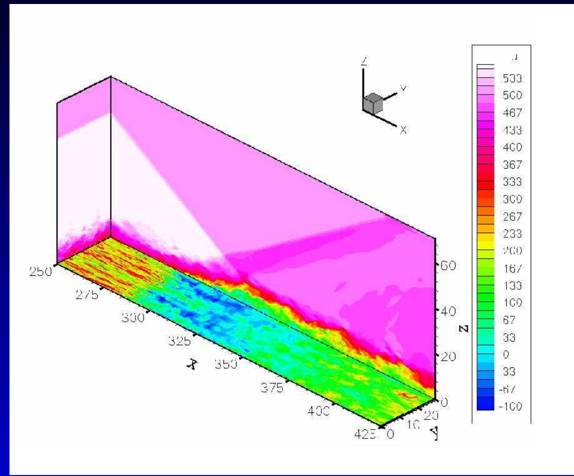

streamwise velocity, $M_\infty = 2.4$ (Garnier *et al.*, AIAA J., 2002):
4th-order centered conservative / skew-symmetric FV
with local ENO filtering (with Ducros sensor)

3D high-subsonic cavity flow:

$(M = 0.9, Re_H = 1.25\ 10^6, L/H = 4)$ *(Y. Dubief)*,
$\sim$ Tracy & Plentovich (*NASA Tech. Paper 3669*, 1997.)

- Rossiter (R.A.E Tech. Rep. 64037, 1964)

$$f_m = \frac{U_\infty}{L} \frac{(m-\gamma)}{\left(\frac{1}{K} + M_\infty\right)} \qquad (7)$$

with $\gamma = 0.25$ and $K = 0.57$ for $L/H = 4$.

m	f_m	tone	$f_m L/U_\infty$	$f_m L/U_\infty$ (Ross.)
1	360 Hz	$\sim F^\sharp$	0.28	0.277
2	820 Hz	$\sim A^\flat$	0.66	0.647
3	1320 Hz	$\sim E$	1.04	1.070

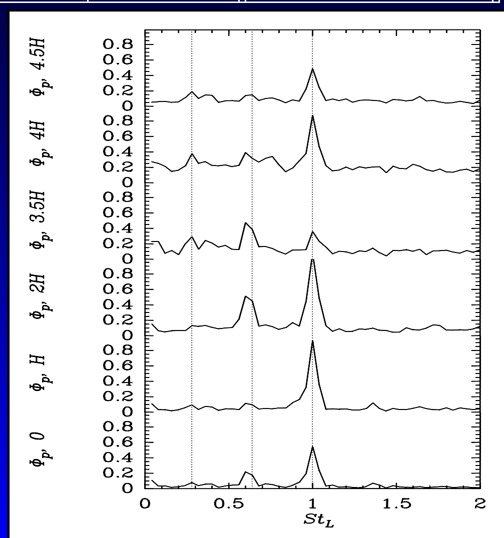

3D high-subsonic cavity flow:

- side view
- perspective
- upstream-looking view

Cavity flow (1/10):

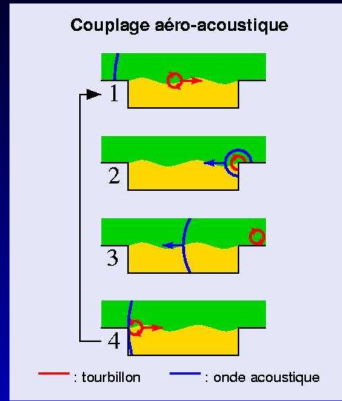

- Rossiter (R.A.E Tech. Rep. 64037, 1964)

$$f_m = \frac{U_\infty}{L} \frac{(m-\gamma)}{\left(\frac{1}{K} + M_\infty\right)} \quad (8)$$

with e.g. $\gamma = 0.25$ and $K = 0.57$ for $L/H = 4$.

Cavity flow (2/10):

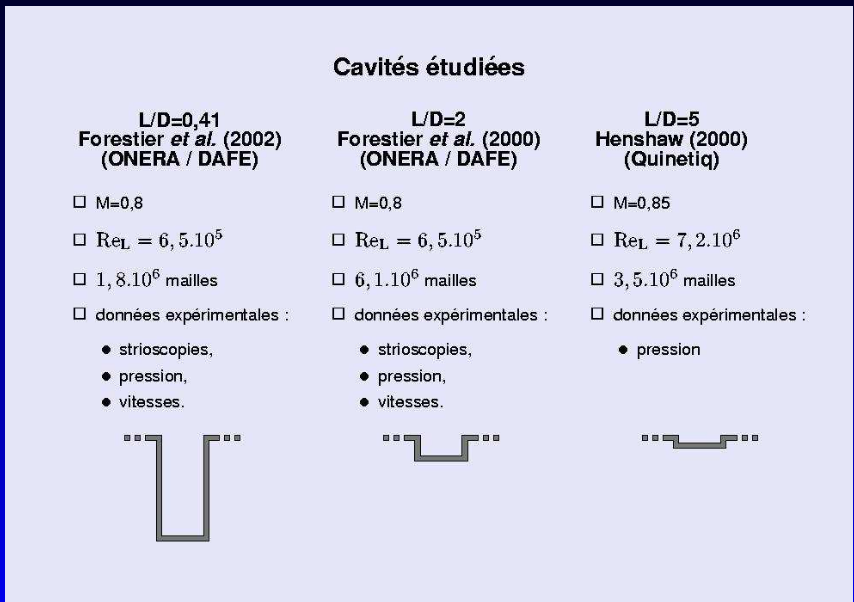

Cavity flow (3/10):

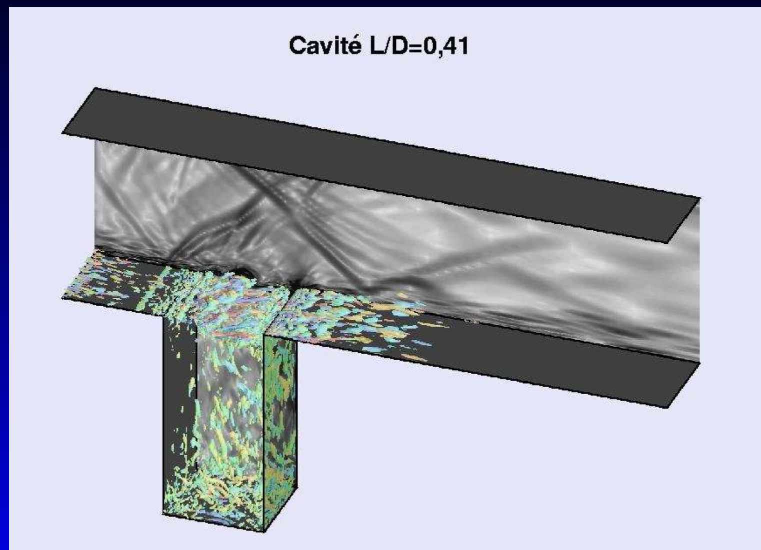

Movies: 1: Schlieren section 2: $Q > 0$ 3: Phase average

Cavity flow (4/10):

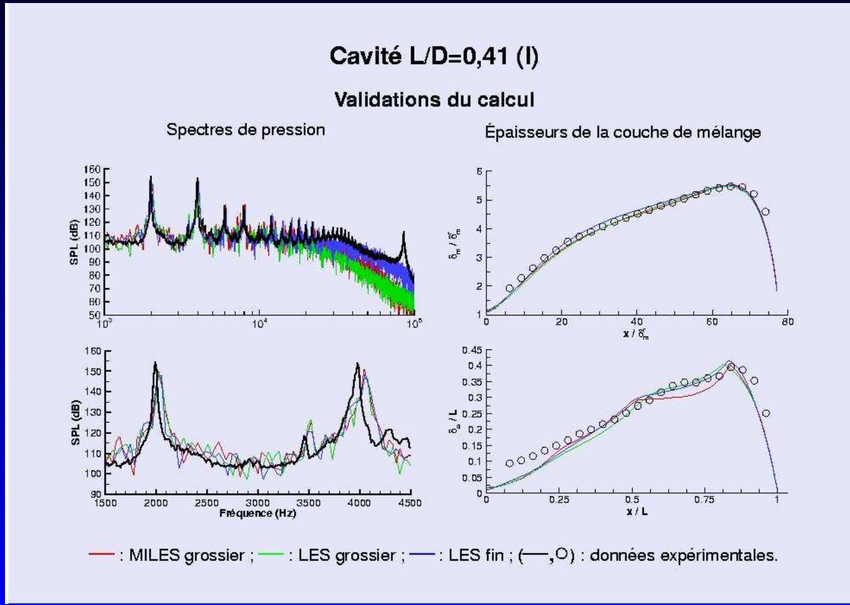

Cavity flow (5/10):

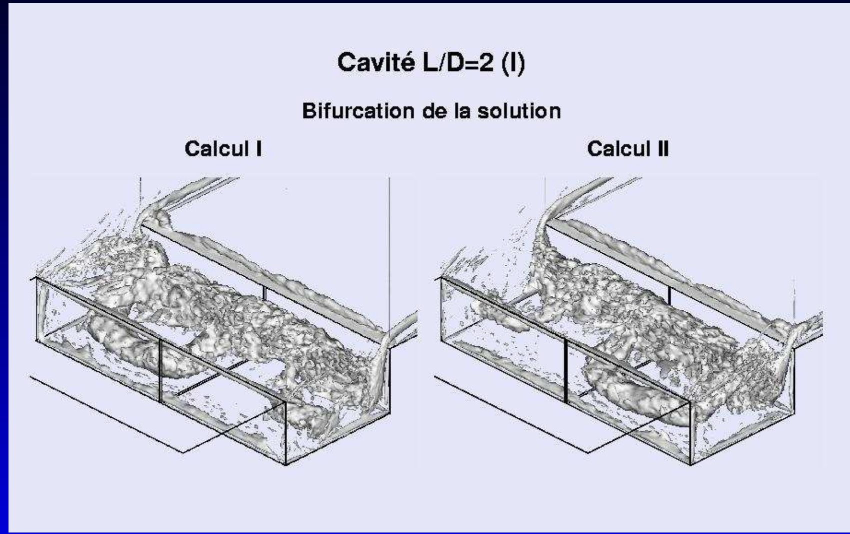

Cavity flow (6/10):

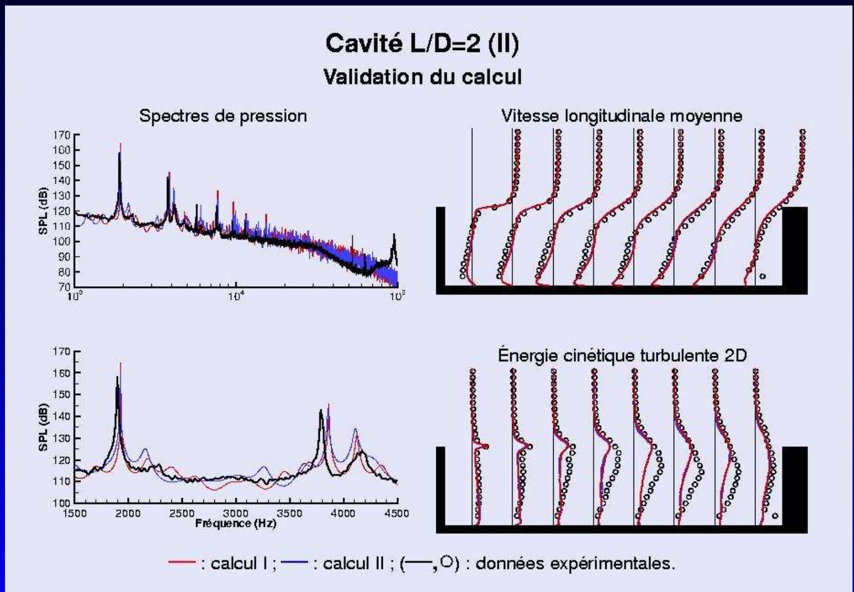

Cavity flow (7/10):

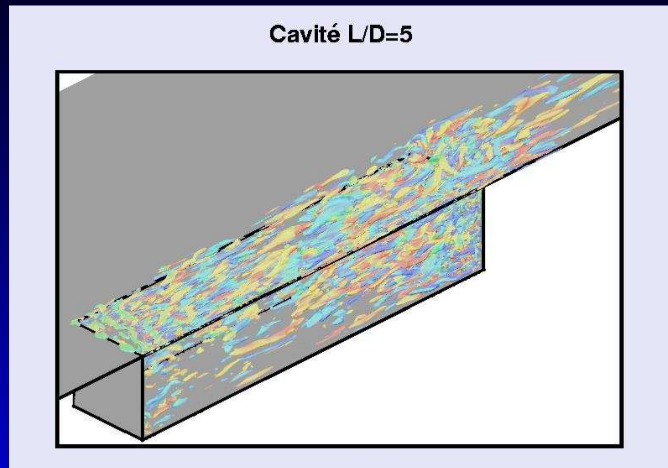

Cavity flow (8/10):

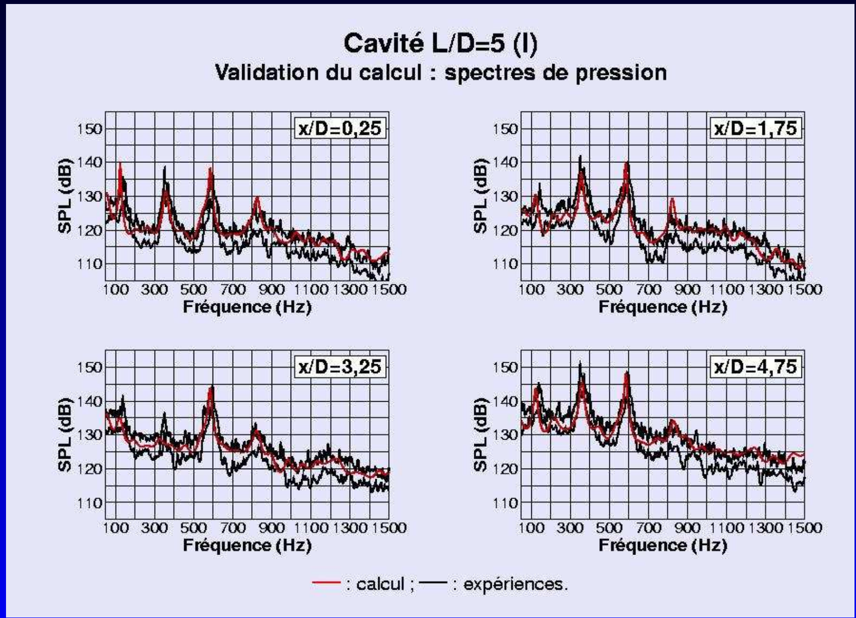

Cavity flow (9/10):

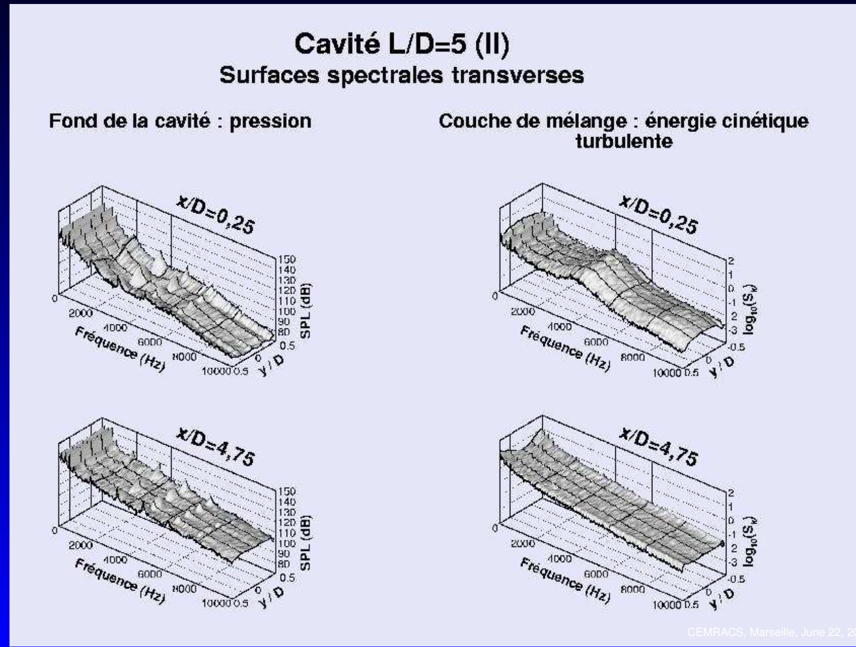

Cavity flow (10/10):

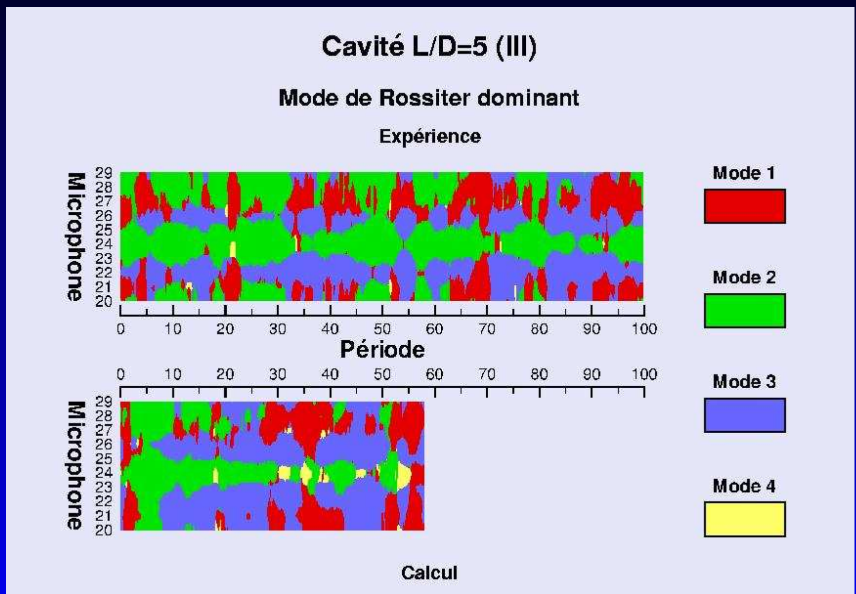

Compression ramps (1/4)

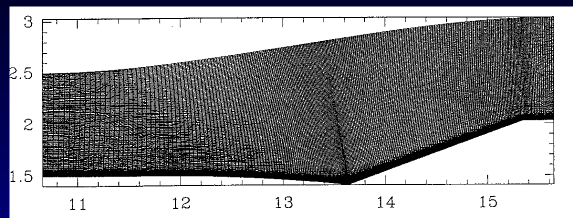

$220 \times 140 \times 25 = 770\,000$ points

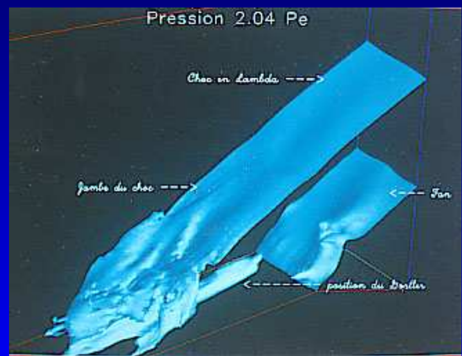

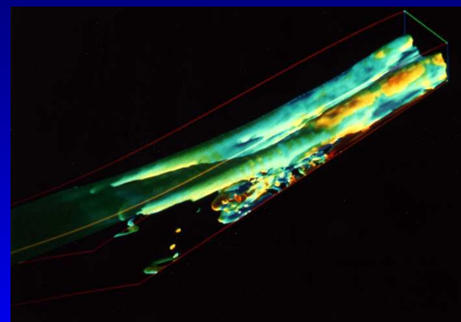

Compression ramps (2/4)

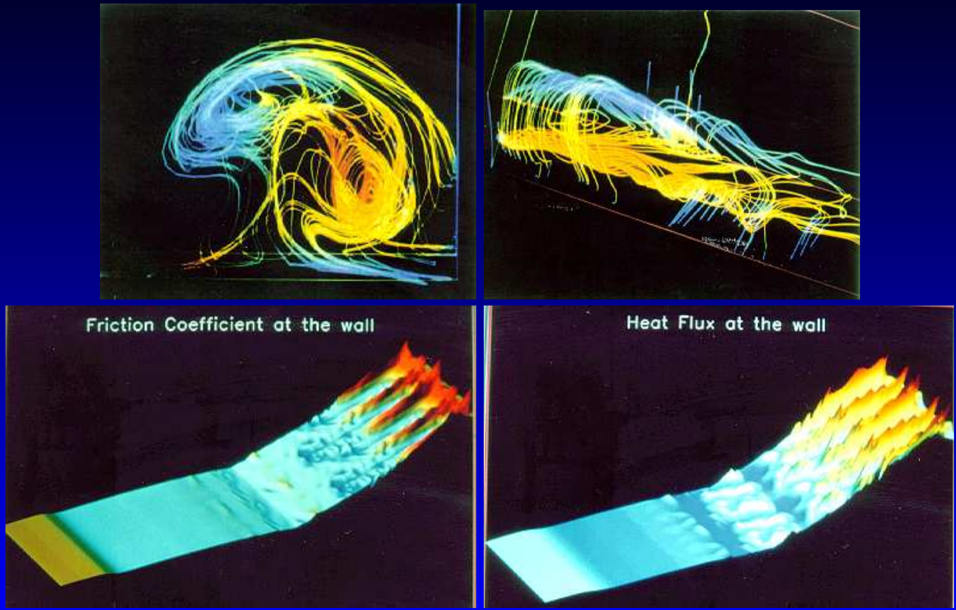

Compression ramps (3/4)

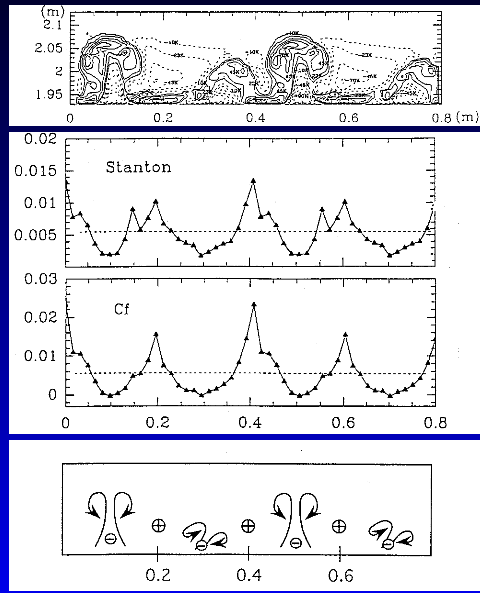

Compression ramps (4/4)

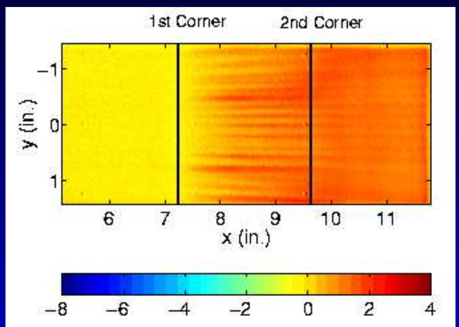

Hyper2000
Thermo Sensitive Paint (above)
heat flux (right)
(Schneider *et al.*, AIAA 2003)

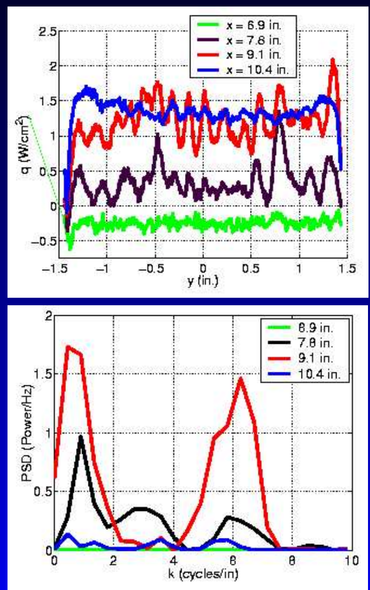

vortex shedding in solid rockets (1 of 4)

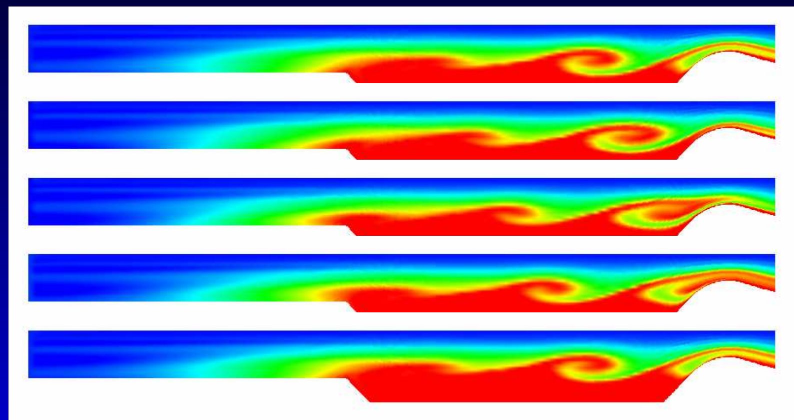

entropy (low Re)

vortex shedding in solid rockets (2 of 4)

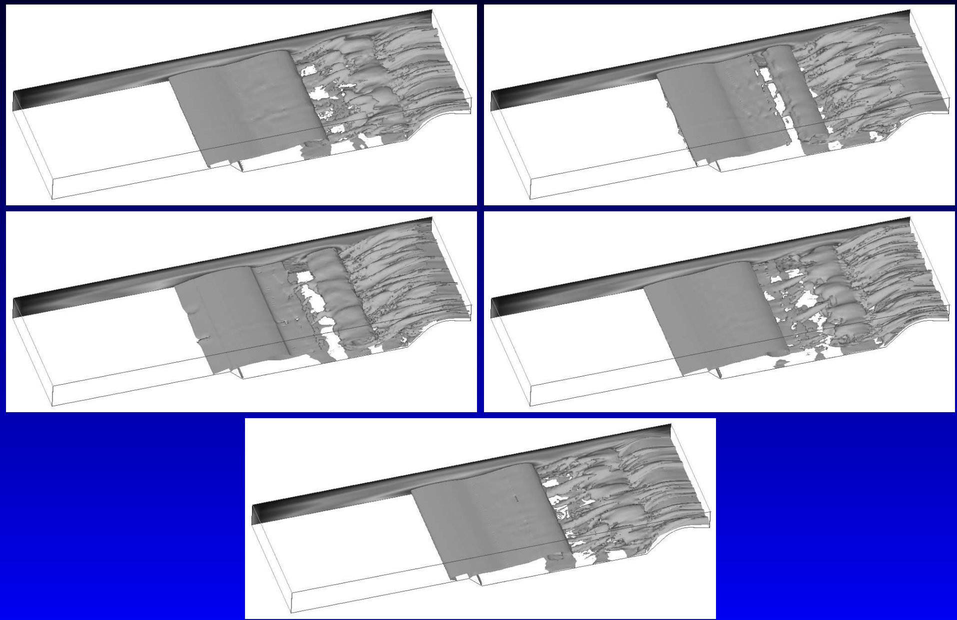

vortex shedding in solid rockets (3 of 4)

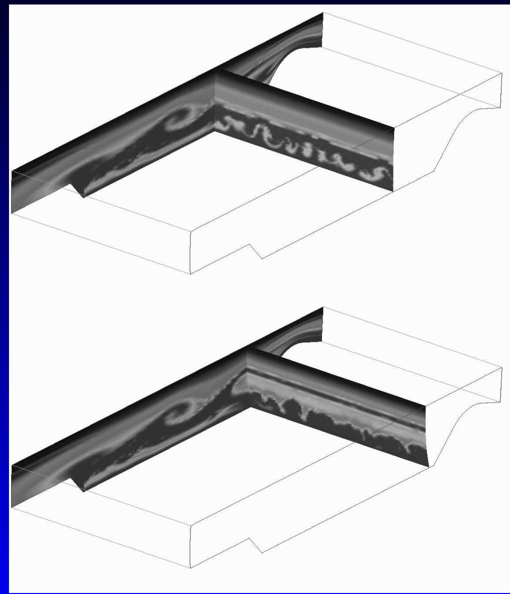

vortex shedding in solid rockets (4 of 4)

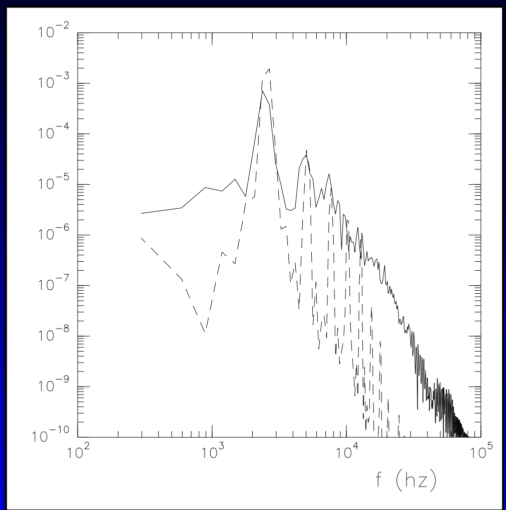

Separation control (preliminary results)

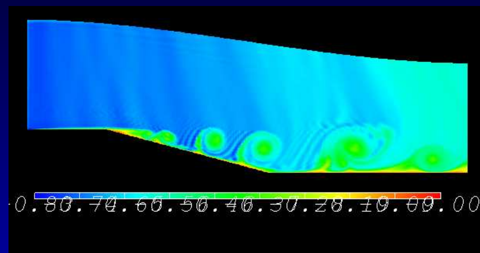

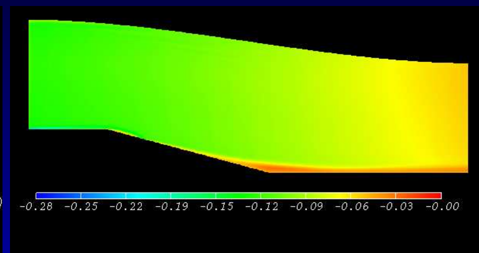

$Re_H = 1000$. Entropy.

Left: no blowing. Right: with tangential blowing.

Supersonic channel flow

- wall friction : $\tau_w = \mu \left.\frac{\partial \tilde{u}}{\partial y}\right|_w = \rho_w u_\tau^2$
- wall heat flux : $q_w = -\lambda \left.\frac{\partial \tilde{T}}{\partial y}\right|_w = -\rho_w C_p u_\tau T_\tau$

$$\rightarrow Re_\tau = \frac{\rho_w u_\tau h}{\mu_w}, \quad M_\tau = \frac{u_\tau}{\sqrt{\gamma R T_w}}, \quad B_q = -\frac{T_\tau}{T_w}$$

DNS references

1. G. Coleman, J. Kim and R.D. Moser *J. Fluid Mech.*, 1995
2. R. Lechner, J. Sesterhenn and R. Friedrich *JoT*, 2001
3. H. Foysi, S. Sarkar and R. Friedrich *J. Fluid Mech.*, 2004

Simulation parameters

case	M	Re	Re_τ	M_τ	$-Bq$	legend
Coleman *et al.* 1995	1.5	3000	222	0.082	0.049	——
	3	4880	451	0.116	0.137	——
Foysi *et al.* 2004	0.3	2820	181	.	.	– –
	1.5	3000	221	.	.	– –
	3	6000	556	.	.	– –
	3.5	11310	1030	.	.	– –
LES	0.3	3000	188	0.018	0.0022	+
	1	"	201	0.057	0.029	○
	1	4880	315	0.055	0.022	×
	1.5	3000	220	0.08	0.05	◁
	2	"	245	0.09	0.08	*
	3	4880	469	0.114	0.137	□
	5	4880	693	0.138	0.28	▽

Mean & RMS streamwise velocity

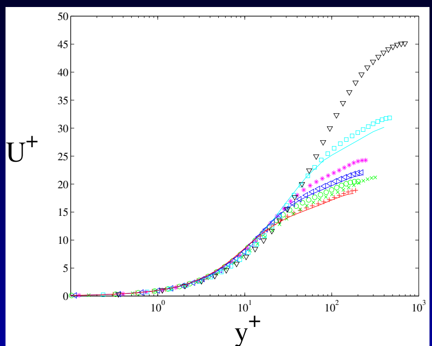

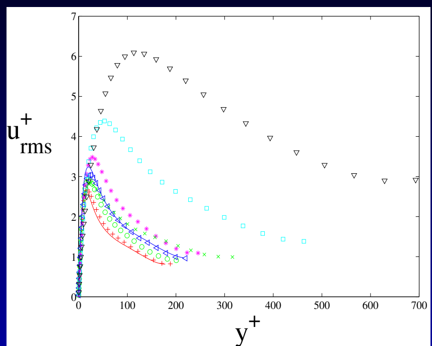

(—— $Mach = 0$ (Kim))

Mean temperature and mean density

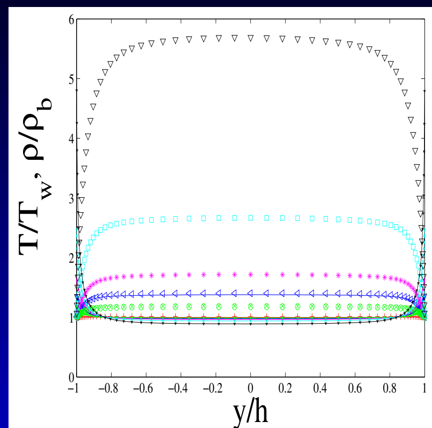

Mach	T_c/T_w	Crocco model
0 (Kim)	1	1
1.5 (Coleman)	1.38	1.42
1.5 LES	1.40	1.42
3 (Coleman)	2.49	2.68
3 LES	2.63	2.68
5 LES	5.7	6.1

compressible Poiseuille flow ‘Crocco-Busemann (1931-1932) type’ relation:

$$\frac{T-T_w}{T_w} = (\gamma - 1)\ Pr\ M^2 \left(\frac{u}{u_b} - 1/3\frac{u^2}{u_b^2}\right)$$

compressibility and viscosity effects

local Mach number

$$M(y) = \frac{\overline{U}}{\sqrt{\gamma R \overline{T}}}$$

local Reynolds number

$$Re(y) = \frac{\rho(\overline{T})\ \overline{U}\ h}{\mu(\overline{T})}$$

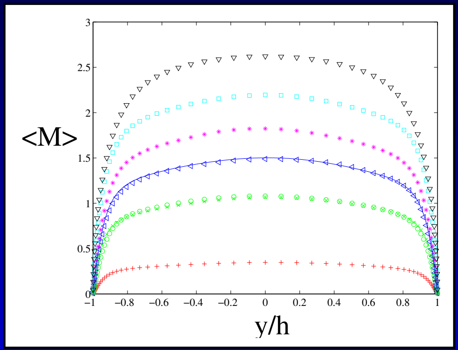

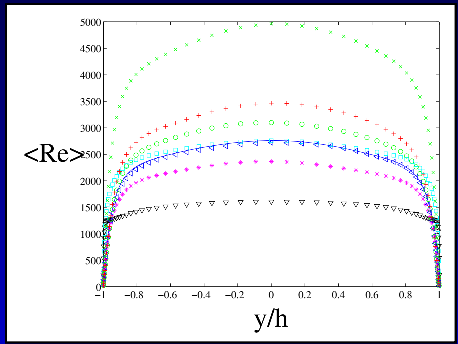

Coherent structures

Q criterion : $Q = \frac{1}{2}\left(\tilde{\omega}_{ij}\tilde{\omega}_{ij} - \tilde{S}_{ij}\tilde{S}_{ij}\right)$

Mach 0.3

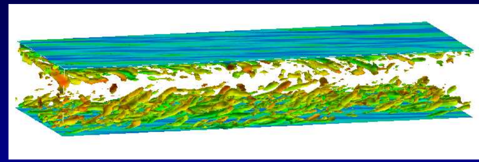

Mach 1.5

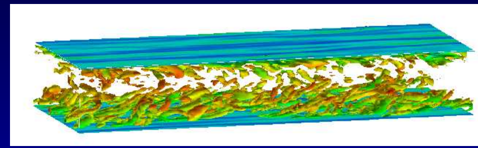

Mach 3

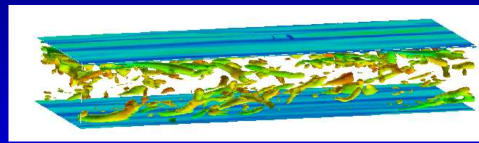

Mach 4

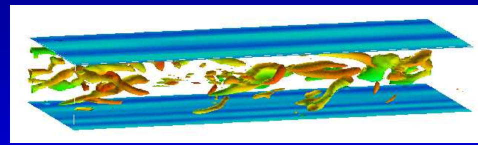

$$Q = 6\frac{u_\tau}{h}$$

Near-wall scaling in fully developed channel flow

Momentum equation

$$\tau_w \approx \mu\frac{\partial \overline{U}}{\partial y} - \rho\ \overline{u'v'}$$

Total Energy equation

$$-q_w \approx \left(\lambda\frac{\partial \overline{T}}{\partial y} - \rho\ \overline{\theta' v'}\right) + \left(\frac{1}{2}\mu\frac{\partial \overline{U}^2}{\partial y} - \rho\ \overline{u'^2 v'}\right)$$

viscous sublayer

$$\rho_w\ u_\tau^2 = \mu\frac{\partial \overline{U}}{\partial y}$$

$$\rho_w\ c_p\ u_\tau\ T_\tau = \lambda\frac{\partial \overline{T_i}}{\partial y} = \lambda\frac{\partial}{\partial y}\left(\overline{T} + \frac{Pr}{2\ c_p}\overline{U}^2\right)$$

(Michel, Quemard & Durand *ONERA N.T.* 1969)

(Debiève, Dupont , Smith & Smits *AIAA J.* 1997)

$$d\overline{U}^+ = \frac{\mu_w}{\mu}\ dy^+$$

$$d\overline{T_i}^+ = Pr\ \frac{\mu_w}{\mu}\ dy^+$$

(Carvin, Debiève & Smits *AIAA J.* 1988)

modified wall unit

$$\overline{U}^+ = \int_0^{y^+}\frac{\mu_w}{\mu}\ dy^+ = y^{c+}$$

$$\overline{T_i}^+ = \overline{T}^+ + \frac{\gamma-1}{2}Pr\ M_\tau^{c2}\ {\overline{U}^+}^2 = Pr\ \ y^{c+}$$

Different wall units

- standard wall units : $y^+ = \frac{\rho_w y u_\tau}{\mu_w}$
- semi-local definitions :
  - ▷ $y_{brad} = \frac{\rho y u_\tau}{\mu}$ (Bradshaw *Ann. Review* 1977)
  - ▷ $y^* = \rho\sqrt{\frac{\tau_w}{\rho}}\frac{y}{\mu}$ (Huang,Coleman,Bradshaw *J. Fluid Mech.* 1995)
- modified wall units : $y^{c+} = \int_0^{y^+}\frac{\mu_w}{\mu}dy^+$

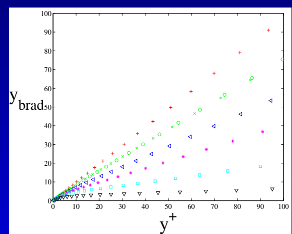

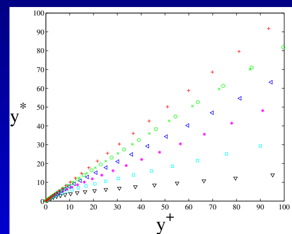

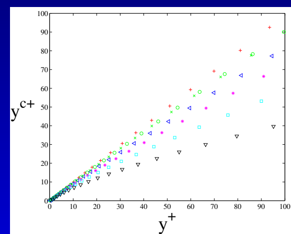

modified flow parameters

Case	Re_b	Re_τ	R_ν	Re_τ^c	$\frac{M_\tau}{B_q^2}$
Kim *et al.* (1987) Mach=0	2800	180	180	180	
Coleman *et al.* (1995) Mach=1.5	3000	222	151	≈ 180	0.37
Coleman *et al.* (1995) Mach=3	4880	451	151	≈ 200	0.31
Present Study					
Mach=0.3	3000	188	185	186	0.39
Mach=1		200	165	180	0.38
Mach=1.5		220	146	176	0.36
Mach=2		245	128	172	0.35
Mach=1	4880	315	165	282	0.37
Mach=3		468	93	245	0.3
Mach=5		693	75	219	0.26

- $U^+ = f(y^+, M_\tau, B_q, (Pr_t, \kappa, n))$ ($\kappa = C_p/C_v$ and $\mu = T^n$) (Rotta 1960)
- *'The appropriate Reynolds number for scaling at given M_e is $R_{brad} = \sqrt{\frac{\rho_w}{\rho_e}} \frac{u_\tau \delta}{\nu_e}$'* (Bradshaw *Ann. Rev. Fluid Mech.* 1977)

Spanwise correlations : streaks mean-spacing

$y_c^+ = 2.5$

R_{uu}

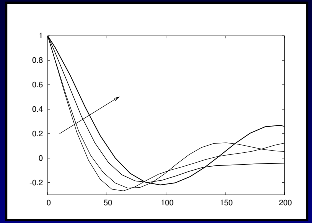

y^+

R_{uu}

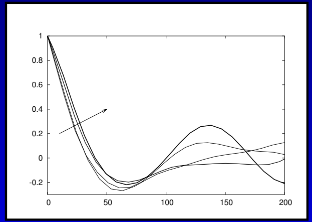

y^{c+}

$\lambda_z^+ \simeq 2y^+(R_{uu_{min}})$

Mach	λ_z^+	$\lambda_{z_c}^+$
0 (Kim)	100	100
0.3	120	130
1	140	130
1.5 (Coleman)	150	≈ 122
1.5	160	140
2	190	140
3 (Coleman)	300	≈ 133

'The Mach number invariance of the integral lengthscale is our most conclusive check on Morkovin's hypothesis at present' (Bradshaw *Ann. Rev. Fluid Mech.* 1977)

Log-scaling in fully developed channel flow

	Momentum equation	Total Energy equation
	$\tau_w \approx -\rho\, \overline{u'v'}$	$-q_w \approx -\rho\, \overline{\theta' v'} - \rho\, \overline{u'^2 v'}$
log region	$\rho_w\, u_\tau^2 = \mu_t \frac{\partial \overline{U}}{\partial y}$	$\rho_w\, c_p\, u_\tau\, T_\tau = \lambda_t \frac{\partial \overline{T_i}}{\partial y} = \lambda_t \frac{\partial}{\partial y}\left(\overline{T} + \frac{Pr_t}{2\, c_p}\overline{U}^2\right)$
mixing length theory	$d\overline{U}^+ = \sqrt{\frac{\rho_w}{\rho}} \frac{1}{\kappa\, y^+} dy^+$	$d\overline{T_i}^+ = \sqrt{\frac{\rho_w}{\rho}} \frac{Pr_t}{\kappa\, y^+} dy^+$
van Driest transform	$\overline{U}_{VD}^+ = \int_0^{\overline{U}^+} \sqrt{\frac{\rho}{\rho_w}}\, d\overline{U}^+ = \frac{1}{\kappa}\, ln\, y^+ + C$ (Van Driest 1955)	$\overline{T}_{iCDS}^+ = \int_0^{\overline{T_i}^+} \frac{1}{Pr_t} \sqrt{\frac{\rho}{\rho_w}}\, d\overline{T_i}^+ = \frac{1}{\kappa}\, ln\, y^+ + C_3$ (Carvin, Debiève & Smits *AIAA* 1988)
Alternative transform	$\overline{U}^{c+} = \int_0^{\overline{U}^+} \frac{y^+}{y^{c+}} \frac{\mu_w}{\mu} \sqrt{\frac{\rho}{\rho_w}}\, d\overline{U}^+ = \frac{1}{\kappa}\, ln\; y^{c+} + C_U^c$	$\overline{T_i}^{c+} = \left[\overline{T}^+ + \frac{\gamma-1}{2} Pr_t\, M_\tau^{c2}\, \overline{U}^{+2}\right]_c = \frac{Pr_t}{\kappa}\, ln\; y^{c+} + C_{T_i}^c$

law of the wall for the mean velocity

van Driest Transformation
density correction

Alternative Transformation
density & viscosity correction

logarithmic zones :

$\overline{U}_{VD}^+ = \frac{1}{\kappa} ln\, y^+ + C$

$\overline{U}^{c+} = \frac{1}{\kappa} ln\, y^{c+} + C_U^c$

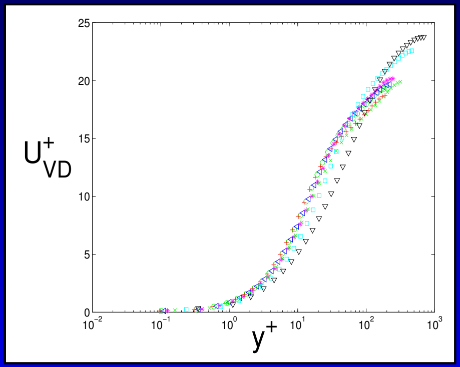

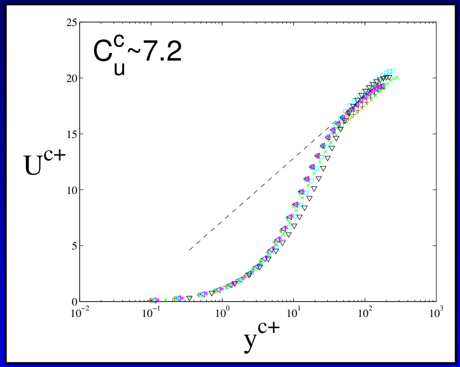

law of the wall for the mean total temperature

van Driest Transformation
density correction

Alternative Transformation
density & viscosity correction

logarithmic zones :

$\overline{T}^{+}_{iCDS} = \frac{1}{\kappa} ln\, y^+ + C_3$

$\overline{T_i}^{c+} = \frac{Pr_t}{\kappa} ln\, y_c^+ + C^c_{T_i}$

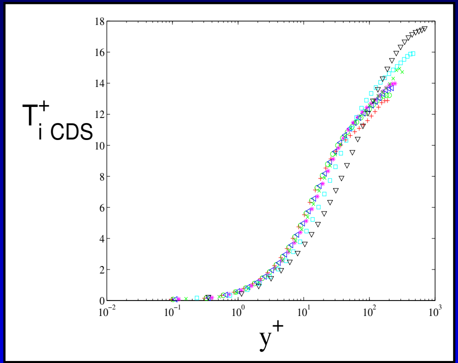

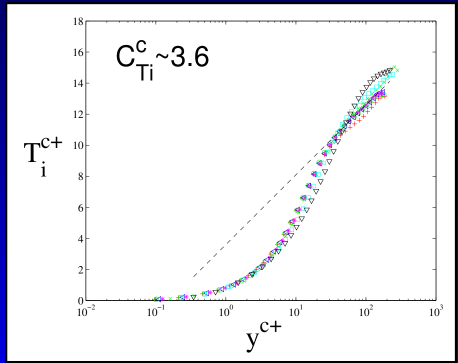

(Michel *et al.* 1969) : $C_3 \approx 3.6$

(Debiève *et al.* 1997) : $C_3 \approx 3$

MHD jets:

I. Motivation : observations

*Examples of observed jets from young stellar object (YSO) and active galactic nuclei (AGN) :
remarkable stability over long distances with respect to the radial extents (~ a few 100 Rj)

These well collimated flows terminate in a strong shock with the external medium (the sonic Mach number is Ms >> 1)

How such supersonic jets survive instabilities ?

YSO

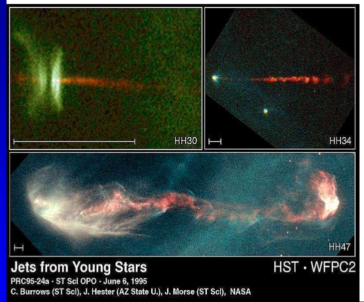

AGN

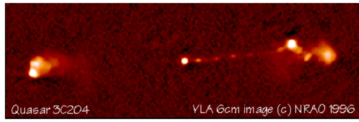

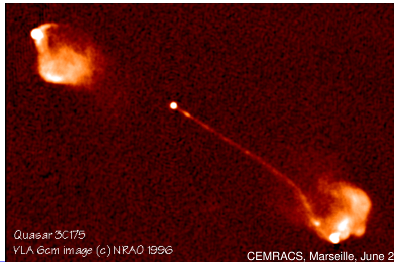

MHD jets:

I. Motivation : theory

*Most high resolution simulations of supersonic flows : **rapid disruption** due to Kelvin-Helmholtz (KH) instabilities (~ 10 Rj
(driven by the velocity difference jet/external medium)

-Hydrodynamic: **turbulent transition** in 3D
Bodo et al. 1998, A&A 333, 1117 (temporal approach)

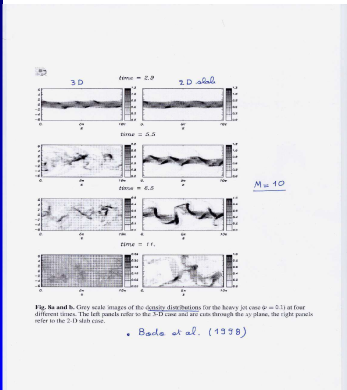

-MHD: most results and conclusion are similar for magnetized jets except in a paper where
*an azimuthal magnetic field component has a significant stabilizing effect !
Rosen et al. 1998, ApJ 510, 136 (spatial approach)

***Helical fields must be considered** (simulations of jet launching from an accretion disk by Casse & Keppens 2004, ApJ 601, 90)

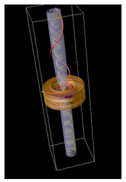

-Other attempts to stabilize KH modes :
jet densities >> surrounding medium density
and/or
favorable radiative effects (critically dependent on the choice of the cooling function)
Downes & Ray 1998; Micono et al. 2000; Stone et al. 1997

How an helical magnetic field affect the MHD instabilities ?
Why an azimuthal component is stabilizing ?
↙ could reduce the discrepancy with observations

MHD jets:

III. Conclusion

- The presence of an helical magnetic field is not sufficient to linearly stabilize the jets
- Presence of Kelvin-Helmholtz (Surface and eventually Body modes) + (magnetic) current-driven instabilities ↙ develop on a fast (linear) time scale ! but are they disruptive ?
- The clue of the remarkable stability in observations could be in the nonlinear effects:
  ↙ has began to be investigated only recently (need an efficient shock capturing code like VAC)

2 examples (recent studies supported in part by Platon)

axial field helical field

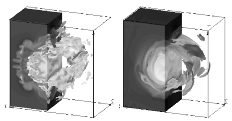

Cylindrical jet with transmagnetosonic flows:
axial velocity + Vz = 0

3D simul.. with VAC and resolution 200*200*100

Axial and longitudinal cuts (density maps)

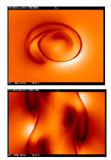

Stabilizing interplay between CD and KH instabilities ↙ less disruptive for the flow

See Baty & Keppens 2002, ApJ 580, 800

Using AMRVAC in 2D (grid adaptive version of VAC) and resol. 1600*1600

Large-scale coalescence + small-scale reconnection events (KH vortices are disrupted)

actually extending to 2D and 3D jets …

Single transonic shear flow layer
extended domain

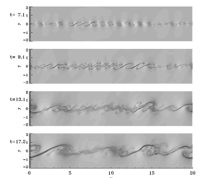

See Baty , Keppens, Comte, 2003, Phys. Plasmas 10, 4661

MHD mixing layers:

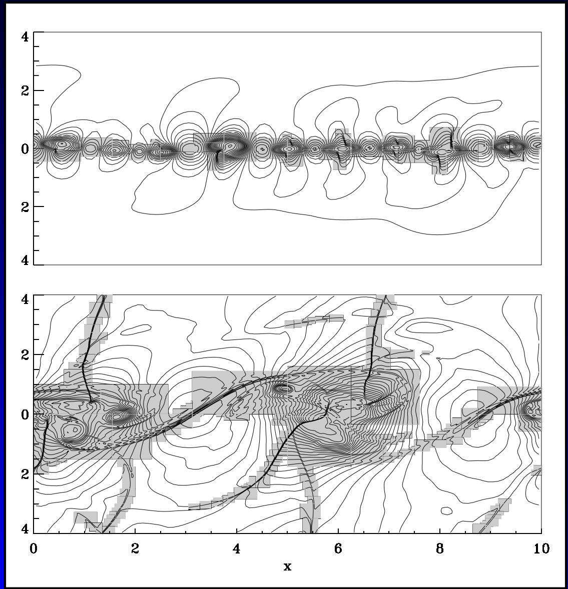

MHD mixing layers:

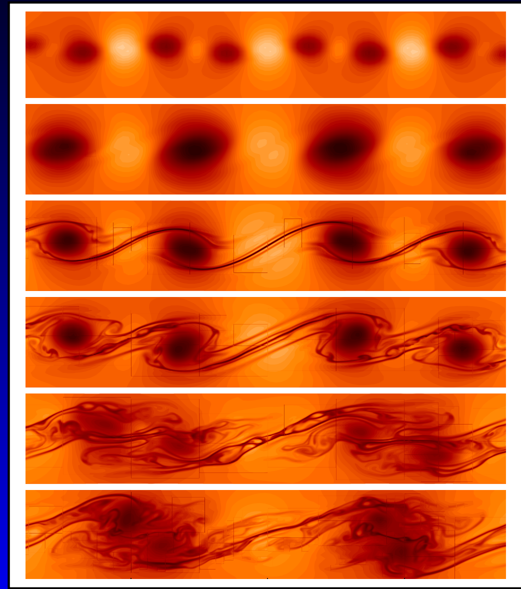

MHD jets:

- $R/m = 10$ ("top hat" initial profile)
  - ▷ without magnetic field
  - ▷ with magnetic field (disruptive regime)
- $R/m = 2$ ($\sim$ jet de Bickley)
  - ▷ without magnetic field
  - ▷ with magnetic field (disruptive regime)

Summary:

- Mixing layers
  - ▷ receptivity to unexpected forcings (helical pairings)
  - ▷ ribs' pairings (despite isotropy assumptions in SGS models)
- Cavity flows
  - ▷ complexity of the acoustic feedback
  - ▷ reflections of acoustic waves $\longrightarrow$ vortex shedding
  - ▷ mean-flow bifurcations
  - ▷ mode switching
  - ▷ influence of aspect ratios $(L/D, L/W)$
- Görtler vortices in external and internal flows
- Supersonic channel flow
  - ▷ possible (non-local) integral scale ?
  - ▷ yet another SRA for non-adiabatic walls
- MHD shear flows: interplay between CD and KH instabilities

Announcements:

- Books:
  - ▷ Lesieur, M., Métais & Comte, P. 2005 Large-Eddy Simulation of Turbulence, *Cambridge University Press*, available in August.
  - ▷ Smits, A.J. & Dussauge, J.-P. 2005 *Turbulent shear layers in supersonic flow.* AIP Press, 2e edition.
- Summer School:
  - ▷ *Turbulence and Mixing in Compressible Flows*
    ERCOFTAC SIG 4, AFM & CNRS
    Strasbourg, July 7-11, 2005
    http://cfd.u-strasbg.fr/SIG4/
- Conference and workshop
  - ▷ *Turbulence and Interactions*
    Porquerolles, May 29 - June 2, 2006
    http://www.onera.fr/congres/ti2006/